Mechanistic Differences between Linear vs Spirocyclic Dialkyldiazirine Probes for Photoaffinity Labeling

Jessica G. K. O'Brien,[#] Louis P. Conway,[#] Paramesh Ramaraj, Appaso M. Jadhav, Jun Jin, Jason K. Dutra, Parrish Evers, Shadi S. Masoud, Manuel Schupp, Iakovos Saridakis, Yong Chen, Nuno Maulide, John P. Pezacki, Christopher W. am Ende*, Christopher G. Parker*, Joseph M. Fox*

# equal contributions

Abstract

Dialkyldiazirines have emerged as a photo-reactive group of choice for interactome mapping in live cell experiments. Upon irradiation, 'linear' dialkyldiazirines produce dialkylcarbenes which are susceptible to both intramolecular reactions and unimolecular elimination processes, as well as diazoalkanes, which also participate in intermolecular labeling. Cyclobutylidene has a nonclassical bonding structure and is stable enough to be captured in bimolecular reactions. Cyclobutanediazirines have more recently been studied as photoaffinity probes based on cyclobutylidene, but the mechanism, especially with respect to the role of putative diazo intermediates, was not fully understood. Here, we show that photolysis (365 nm) of cyclobutanediazirines can produce cyclobutylidene intermediates as evidenced by formation of their expected bimolecular and unimolecular products, including methylenecyclopropane derivatives. Unlike linear diazirines, cyclobutanediazirine photolysis in the presence of tetramethylethylene produces a [2+1] cycloaddition adduct. By contrast, linear diazirines produce diazo compounds upon low temperature photolysis in THF, whereas diazo compounds are not detected in similar photolyses of cyclobutanediazirines. Diazocyclobutane, prepared by independent synthesis, is labile, reactive toward water and capable of protein alkylation. The rate of diazocyclobutane decomposition is not affected by 365 nm light, suggesting that the photochemical conversion of diazocyclobutane to cyclobutylidene is not an important pathway. Finally, chemical proteomic studies revealed that a likely consequence of this primary conversion to a highly reactive carbene is a marked decrease in labeling by cyclobutanediazirine-based probes relative to linear diazirine counterparts both at the individual protein and proteome-wide levels. Collectively, these observations are consistent with a mechanistic picture for cyclobutanediazirine photolysis that involves carbene chemistry with minimal formation of diazo intermediates, and contrasts with the photolyses of linear diazirines where alkylation by diazo intermediates plays a more significant role.

Introduction

Photoaffinity labeling is a broadly used technique used to interrogate interactions between small molecule ligands and their biological targets in living cells.[1-4] Photoaffinity probes are constructed by attaching a ligand to an enrichment handle (e.g. an alkyne or biotin) as well as a photoreactive group, which upon excitation generates a short-lived reactive intermediate capable of capturing proximal targets. Classically, aromatic diazirines, arylazides, and benzophenone analogs have employed for the construction of photoaffinity probes.[3, 5] More recent probes based on aryl carboxytetrazoles,[6] pyrones,[7] pyrimidones,[7] and photoredox catalysis[8] offer alternatives to conventional methods for photoaffinity labeling.

Ideally, a photoaffinity probe will display permeability and binding properties that are nearly identical to the parent probe, and upon photolysis will crosslink targets with high yield and extremely rapid kinetics, thereby enabling effective mapping of the target and interactome.[9] Effective photoaffinity probes should also be capable of activating at wavelengths and operating under photolysis conditions that do not cause cytotoxicity or damage to the cellular targets under study. Additionally, the size and lipophilicity of the photoaffinity label should ideally be minimized in order to avoid negative effects on the function, solubility, permeability, and subcellular localization of the biological molecules under investigation.

In practice, it can be difficult to include all of the above-mentioned properties in a single probe. Classical probes based on benzophenones, aryl azides, and aryl diazirines display favorable crosslinking kinetics, but their large size and hydrophobicity can dominate the physicochemical properties of the probe.[3, 5] Because of their minimal size and favorable physicochemical properties, dialkyldiazirines have emerged as photoaffinity probes for a range of cellular interactions, including small molecule-protein interactions,[9, 10] including drugs,[11] natural products,[12] and fragments,[13] as well as protein-protein interactions,[14] nucleic acid-protein interactions,[15] metabolic oligosaccharide engineering,[16] lipid-protein interactions,[17] and the study of biological membranes.[18]

The bimolecular capture of biological targets by diazirines during photoaffinity labeling is commonly attributed to carbene insertion processes. While this is the case for α-trifluoromethyl-α-phenyldiazirine,[19] the situation is different for aliphatic diazirines. Diazirines produce both diazo compounds and carbene products upon irradiation.[19, 20] However, alkylcarbenes from aliphatic diazirines can undergo rapid intramolecular rearrangements with α-hydrogens, potentially limiting their ability to engage intermolecular targets.[21-27] Meanwhile, aliphatic diazo compounds are reactive, and can undergo protonation at neutral pH to produce reactive diazonium compounds.[28] The resulting diazonium salts are alkylating agents that can crosslink intermolecular targets,[29] but with kinetics that are much slower than carbene crosslinking.[30, 31] Alkyldiazonium ions are therefore likely to have a substantially greater labeling radius than more reactive carbene intermediates in biological target identification investigations. Additionally, alkyldiazonium ions are likely to alkylate carboxylic acid residues when they do react with proteins to give ester bonds that could then be susceptible to hydrolysis by esterases in proteomic workflow and live cell assays.[29, 32-34]

In classic studies, Kirmse and Platz used competition experiments to understand the relative contributions of carbene and diazo intermediates in the photochemistry of diazirines fused to

norbornane and bicyclo[2.1.1]hexane.[27] Recently, we studied the photochemistry of linear dialkyldiazirines of the type commonly used in biological labeling.[35] Deuterium labeling and diazo compound trapping experiments were employed to demonstrate that both carbene and diazo mechanisms operate, as well as a secondary alkylation process derived from a carbonyl ylide. It was shown that the carbene mechanism was primarily responsible for intramolecular alkene products, whereas bimolecular products are largely due in large part to alkylation chemistry (Fig 1A). As discussed above, the mechanistic details have implications for chemical biology applications since carbene insertion reactions display different chemoselectivity and are substantially faster than alkylations of diazonium or oxocarbenium ions. Recently, Woo and coworkers evaluated the labeling preferences of alkyl and aryl diazirines.[36] Consistent with the formation of diazo intermediates, they observed that alkyldiazirines exhibit preferential labeling of acidic amino acids in a pH-dependent manner and in live cells preferentially enrich highly acidic proteins or those embedded in membranes.

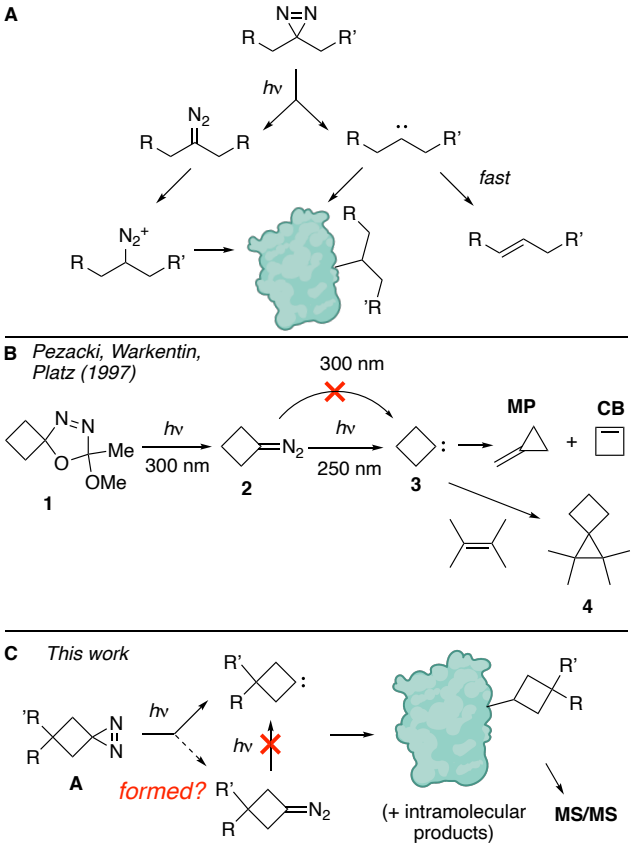

Figure 1. (A) 'Linear' diazirines produce both carbenes and diazo compounds upon photolysis. The carbene products are susceptible to intramolecular 1,2-H-shift. A primary labeling pathway involves protonation of the diazo compound and subsequent alkylation. (B) Prior studies showed spirocyclic oxadiazoline ketal **1** to be a precursor to diazocyclobutane **2**, which can be used to produce cyclobutylidine **3** at 250 nm irradiation, but not at wavelengths longer than 300 nm with standard light sources. (C) We demonstrate that cyclobutanediazirines **A** produce carbene products upon photolysis. The diazocyclobutane is not observed, and does not serve as a photochemical precursor to the carbene.

While linear dialkylcarbenes are susceptible to intramolecular rearrangement, observation of bimolecular reactions of alkylcarbenes in conformationally constrained systems is well documented.[23, 37, 38] The smallest and perhaps simplest example of such a system is cyclobutylidene (**3**), which has been studied since 1960[37, 39-42] was first shown to undergo intermolecular 2+1 cycloaddition to give bicyclohexane products as early as 1984.[42] Calculations predict that cyclobutylidene has a nonclassical carbene structure stablized via transannular interaction of the distal methylene group. Reflective of higher singlet stability in the nonclassical structure in cyclobutylidene is a computed singlet–triplet energy gap that favors the singlet excited state by 5.9 kcal/mol as compared to a singlet-triplet gap of only 1.3 kcal/mol for dimethylcarbene.[43] Pezacki, Warkentin

and Platz showed that cyclobutylidene could be generated from the laser flash photolysis (LFP, 308 nm) of oxadiazoline ketal **1**.[37] Unlike the 308 nm LFP result, conventional irradiation of **1** at 300 nm with UV-B bulbs was shown to produce diazocyclobutane **2** without the formation of carbene products. The difference was attributed to multiphoton excitation in the LFP method which does not occur in conventional photolysis. It was shown that diazocyclobutane **2** does not react thermally with tetramethylethylene to give 4,4,5,5-tetramethyl[2.3]spirohexane (**4)** via a 3+2/loss of nitrogen mechanism. However, carbene **3** can be generated via 250 nm irradiation and trapped by tetramethylethylene to give spirocyclohexane **4** in 21% yield. Also produced are methylenecyclopropane (**MP**) as the major intramolecular product and cyclobutene (**CB**) as a minor product.[37] **MP** is essentially the major product from carbene **3**, whereas the excited state of diazocyclobutane **2** gives a 3.6:1 mixture of **MP**:**CB**. In agreement with experimental studies, computational investigations also predict that 1,2-carbon shift to give **MP** is an order of magnitude faster than 1,2-hydrogen migration to give **CB**, and three orders of magnitude faster than 1,3-hydrogen migration to give cyclobutane.[44]

Given these precedents, we hypothesized that spirocyclic diazirines **A** could serve as minimal probes capable of photoaffinity labeling through a 'true' carbene mechanism (Figure 1C). Described in this study are demonstrations that these 'cyclobutanediazirines'[45] produce bimolecular and unimolecular products consistent with carbene intermediates.

Functionalized spirocyclic diazirines, including cyclobutanediazirine, were first reported in 2019 by Grygorenko and coworkers.[46] In the course of our studies, Woo and coworkers described cyclobutanediazirines for applications in live cell photocrosslinking.[47] They found that cyclobutanediazirines can label protein targets in cells and be utilized to map small molecule−protein binding sites, albeit with a significant reduction in labeling of targets. Mechanistically, cyclobutanediazirines were proposed to partition between diazocyclobutane and carbene intermediates. Cyclobutane diazirines displayed labeling that was less pH-dependent and a different reactivity profile relative to linear diazirine tags, and carbene labeling was proposed as the major bimolecular pathway. Diazocyclobutanes were proposed to undergo further photochemical transition to carbenes, rather than protonation/alkylation as has been described for linear carbenes. Only cyclobutene products were described as intramolecular byproducts of cyclobutanediazirine photolysis, whereas the methylenecyclopropane products expected from a carbene pathway were not described.

As discussed below, we propose a differing model of cyclobutanediazirine photolysis where the diazirine serves as the sole source of carbenes. Diazocyclobutanes are not observed in low temperature photolyses of a cyclobutanediazirine, whereas low temperature photolyses of linear diazirines do produce diazo compounds. Diazocyclobutane was prepared independently and shown to be thermally labile, and reactive toward water. Diazocyclobutanes are shown not to be photochemical precursors to carbenes upon illumination with UV-A (365 nm) light. Consistent with the formation of carbenes from cyclobutanediazirine photolysis, trapping with tetramethylethylene led to a cyclopropane product, and methylenecyclopropanes are observed as the major unimolecular rearrangement product of cyclobutyl diazirine photolyses along with the minor formation of cyclobutene products. Cell-based fluorescence and proteomics experiments demonstrated a marked reduction in labeling by the cyclobutyldiazirine-based probes compared to their linear diazirine counterparts, consistent with previous reports .[47]

Results and Discussion

Synthesis

As standards for mechanistic studies with cyclobutanediazirines, we prepared benzylester and benzylamide analogs of methylenecyclopropanes, cyclobutenes, bicyclobutane, and **Figure 2.**

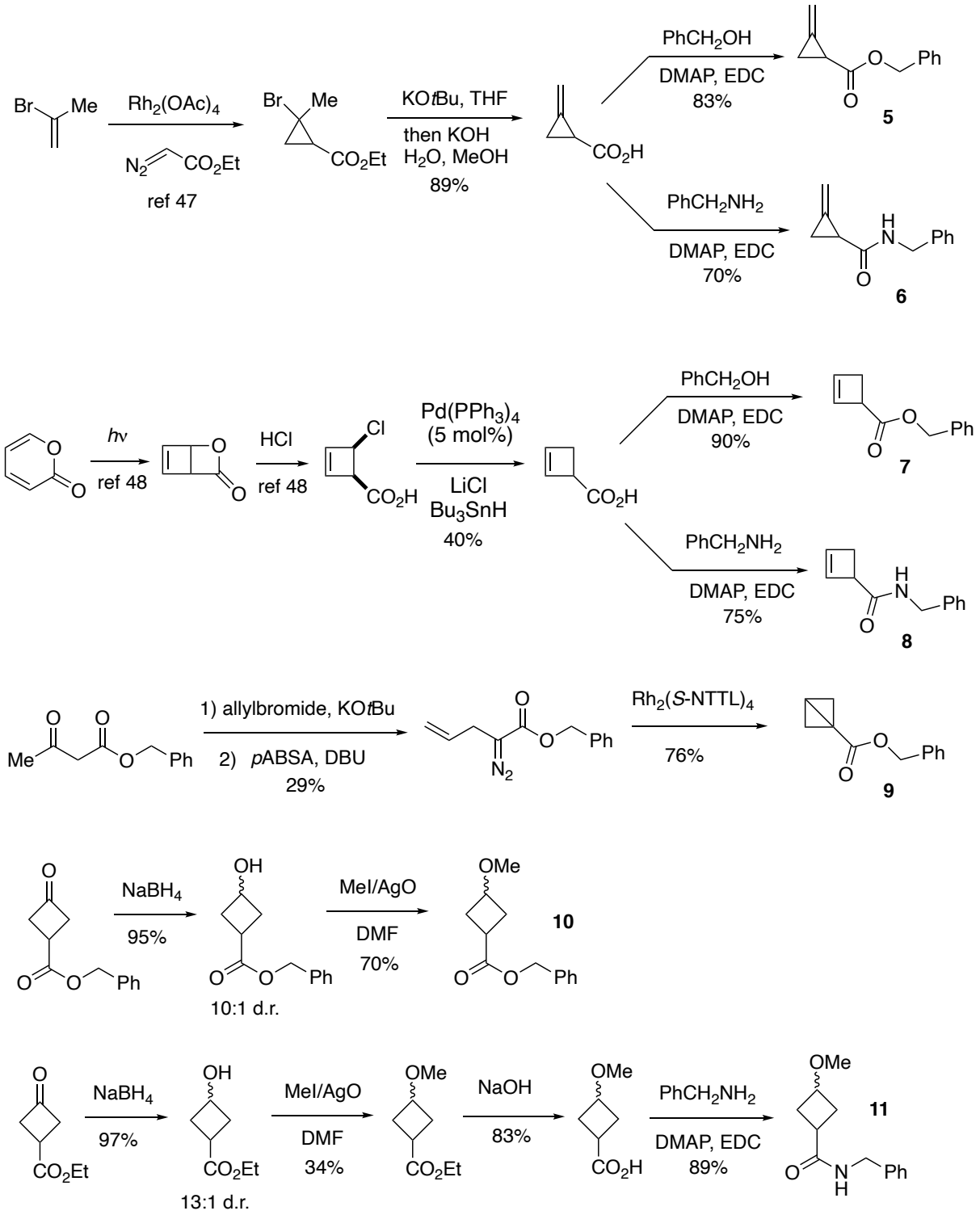

Figure 2. Synthesis of standards for mechanistic studies

cyclobutylmethylether product. Cyclopropanation,[48] dehydrohalogenation, and EDC/DMAP coupling provided access to methylenecyclopropanes **5** and **6**. Cyclobut-2-ene carboxylic acid was prepared from *cis*-4-chloro-cyclobutenecarboxylic acid[49] and served as precursor to ester **7** and amide **8**. Benzyl bicyclo[1.1.0]butane-1-carboxylate **9** was prepared from benzyl acetoacetate by a sequence of allylation, diazo transfer, and intramolecular cyclopropanation.[50] Cyclobutylmethylethers **10** and **11** were prepared as ≥10:1 syn:anti mixtures of diastereomers, using a sequence of $NaBH_4$ and AgO/MeI mediated methylation as key steps.

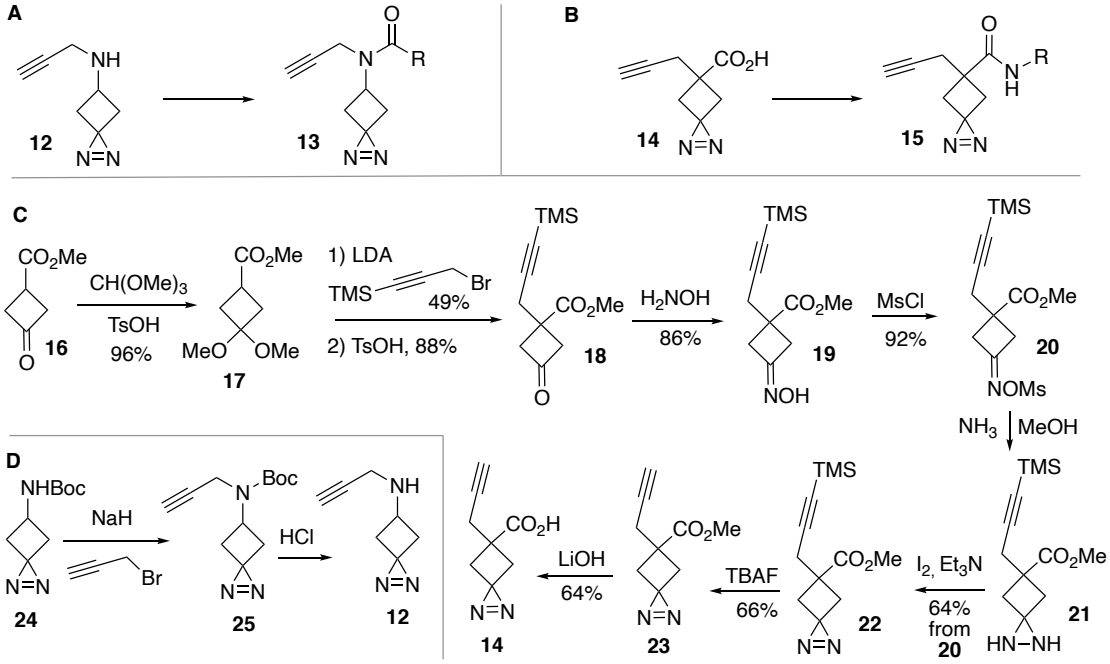

Figure 3. Synthesis of alkyne-functionalized cyclobutanediazirines

As functionalized precursors to cyclobutylidienes, we synthesized a series of probes based on the alkyne-functionalized spirocyclic diazirines: *N*-(propynyl)-1,2-diazaspiro[2.3]hex-1-en-5-amine (**13**) and 5-propynyl-1,2-diazaspiro[2.3]hex-1-ene-5-carboxylic acid (**15**) (Fig 5A,B). Straightforward acylation reactions converted **12** and **14** into structural analogs **13** and **15**, respectively. Compound **14** was synthesized from methyl 3-oxocyclobutane-1-carboxylate (**16**) through conversion to ketal **17** in 96% yield (Fig 5C). Introduction of a trimethylsilylpropargyl group followed by acid catalyzed deprotection gave **18** in 43% yield after 2 steps. A two-step sequence of oxime formation to give **19** and mesylation gave a 79% yield of **20**, which could be converted to diazirine **22** in 64% yield through sequential treatment with ammonia to give **21** followed by oxidation with iodine. TBAF removed the silyl protecting group to give **22** in 66% yield, and saponification with LiOH gave carboxylic acid functionalized spirocyclic diazirine **23** in 64% yield. The amine-functionalized spirocyclic diazirine **12** was prepared by propargylation of commercially available **24** followed by Boc-deprotection (Fig 5D).

Evidence for carbene chemistry in photolyses of cyclobutanediazirines

While the chemistry of cyclobutylidene has been studied using a variety of precursors, including diazo compounds,[39] tosylhydrazone salts,[41, 42] gem-dihalocyclobutanes,[41, 42] and oxadiazoline ketals,[37] diazirine precursors had not been explored. As the nature of the precursor can have an effect on the relative contributions of carbene vs precursor rearrangement chemistry, we sought to characterize the photolysis products of cyclobutanediazirine derivatives. The synthesis of a series of functionalized spirocyclic diazirines, including cyclobutanediazirine[45], had been reported by Grygorenko and coworkers.[46]

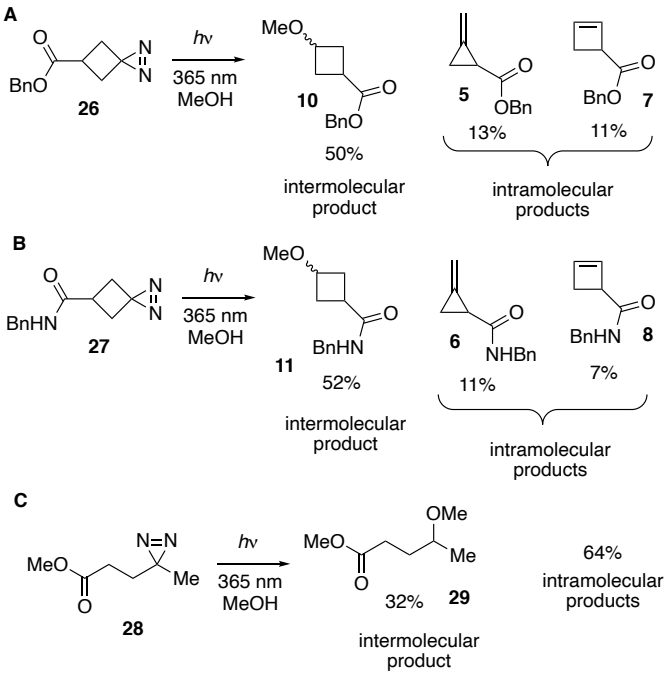

Figure 4 (A,B) Photolysis of spirocyclic diazirines in MeOH produces intermolecular products **10** and **11** in >50% yield, along with methylenecyclopropane and cyclobutene products of unimolecular rearrangement. (C) Photolysis of linear diazirine **28** produces intermolecular product **29** in 32% yield, along with 64% yield of alkene products of unimolecular rearrangement.

As shown in Figure 4, the UV-A photolyses of spirocyclic diazirine **26** in methanol gave rise to 50% of the cyclopropylmethyl ether product **10** as well as methylenecyclopropane **5** (13%) and cyclobutene **7** (11%) (Figure 2A). Benzyl bicyclo[1.1.0]butane-1-carboxylate (**9**, Figure 2) was not observed. Similarly, amide analog **27** led to ether **11**, methylenecyclopropane **6** and cyclobutene **8** in 52%, 11% and 7% yields, respectively (Figure 2B). Yields were measured by ^{1}H NMR and structural assignments were made by comparison to standards that were independently synthesized (Figure 2). Suggestive of contributing carbene chemistry, the yields of the bimolecular MeOH-adducts **10** (50%) and **11** (52%) are higher than the yield of MeOH-adduct **29** (32%) previously described for photolysis of a linear diazirine **28** (Figure 2C).[35] Also consistent with a contributing carbene mechanism is formation of methylenecyclopropanes as the major unimolecular products,[37, 39-42] while the observation of cyclobutene formation indicates that a non-carbene mechanism is also competitive.[37]

We tested whether a carbene intermediate from photolysis of diazirine **26** could be intercepted via alkene cyclopropanation. Earlier studies have shown that 4,4,5,5-tetramethyl[2.3]spirohexane products are derived from the capture of cyclobutylidene, but not from diazocyclobutane.[37] When **26** is irradiated in the presence of 2M tetramethylethylene (TME) in cyclohexane with UV-A light for 120 minutes, carbene trapping adduct **30** was formed in 24% isolated yield. Our result is comparable to the 21% yield obtained by Pezacki et al. for carbene generated via 250 nm photolysis of an oxadiazolone ketal precursor to produce 4,4,5,5-tetramethyl[2.3]spirohexane **4**.[37] Also detected by GC along with **30** were intramolecular rearrangement products methylenecyclopropane **5** and cyclobutene **7**. An analogous photolysis experiment with diazirine **31** in the presence of TME gave the expected intramolecular products but produced ≤2% of cyclopropane **32** by GC analysis (Fig 5B).

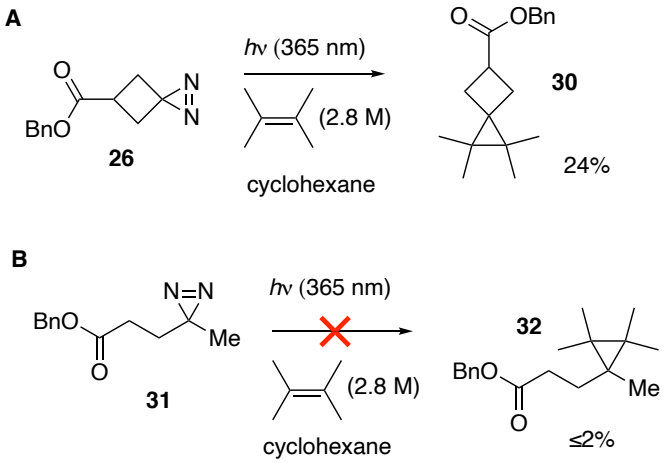

Figure 5 (A) Cyclopropanation with cyclobutanediazirine **26** succeeds, whereas (B) linear diazirine **28** does not give cyclopropane products.

Decomposition of Diazocyclobutane is Accelerated by Water, but not UV-A Light

The irradiation of diazirines with UV-A (365 nm) light may give rise to diazo compounds as well as carbenes.[19, 27, 51] To study whether a diazocyclobutane intermediate could lead to carbene formation, we revisited the Pezacki and Warkentin synthesis of diazocyclobutane (**2**). This was accomplished via UV-B (300 nm) irradiation of 0.1 M solutions of **1** for 15 min in anhydrous THF (Figure 4A). The diazo compound is thermally sensitive and we found it was best prepared by low-temperature photolysis using a –78 °C cold finger. As expected, the diazo compound is bright pink in solution with a low-intensity absorption in the UV-vis at 525 nm.[52]

We measured the decay of the absorption at 525 nm associated with **2** with in situ spectroscopic monitoring at 24 °C in a thermostated cuvette (Fig 4B). The diazo compound is labile and decays in anhydrous THF with an average half-life of 215 seconds (Fig 4C, top right). By comparison, Platz reports the stability of a dichloromethane solution of acyclic dipropyldiazomethane to be more stable ($t_{1/2}$ ~ 1 hour).[51] The half-life of **2** was insensitive to irradiation by UV-A light (365 nm, 20 mW/cm^2) (Fig 1C, middle). This result is consistent with the earlier observations of Pezacki and Warkentin, who found that diazocyclobutane **2** was not affected by 300 nm light, but gave carbene products when photolyzed with 250 nm light.[37] By contrast, **2** is water sensitive. Upon mixing 0.5 mL of a THF solution of **2** with 0.5 mL water or PBS, the pink color disappeared rapidly. In an experiment conducted with in situ monitoring of diazo disappearance, 100 uL water was added to 1 mL of a THF solution of 2-4 (Fig 1C, bottom). Relative to an anhydrous sample, the rate of decomposition increases >3-fold with an average half-life of 63 seconds. This fast reactivity of the diazocyclobutane is consistent with earlier studies on rates

diazonium ion formation via diazocycloalkane protonation under anhydrous conditions, where strain-relief was proposed to explain the faster reactivity of diazocyclobutane relative to diazocyclopentane or diazocyclohexane.[53]

To investigate whether diazocyclobutane (**2**) is capable of non-photochemical protein alkylation, we investigated the reaction of **2** toward bovine serum albumin (BSA) followed by protein digestion and MS/MS analysis (Fig 6D). For these experiments, a high concentration of **2** was utilized to mimic the conditions of proximity labeling. Thus, a 150 μM solution of BSA in ultrapure H_2O was mixed with a solution of **2** in THF which was freshly prepared from **1** (10 mM) by low temperature photolysis as described above. The pink color of **2** quickly dissipated upon mixing accompanied by the evolution of nitrogen gas. After 1 hour, the protein was precipitated, pelleted and resuspended in 50 mM ammonium bicarbonate with 6 M urea. Samples were reduced with DTT, alkylated with iodoacetamide, trypsin digested and then processed for LC-MS/MS analysis. A mass shift of +54 Da corresponding to the addition of a cyclobutane with the loss of 1 proton from the nucleophile was observed on 229 specific unique BSA amino acid side chains. BSA contains 60 lysine, 35 cysteine, 32 serine, 17 histidine, 40 aspartate, and 59 glutamate residues. These residues account for 243 of the 607 amino acids in BSA and represent nucleophilic residues likely to react with the diazocyclobutane; therefore, the addition of +54 Da was screened for and detected on each of these residues. Each of these residues displayed the 54 Da addition with the following percent of unique detected amino acid labeling to amino acid prevalence in BSA: 98% Lys, 94% Cys, 72% Ser, 94% His, 100% Asp, and 98% Glu. The results suggest that, if cyclobutanediazirine photolysis produces diazocyclobutane intermediates, that non-photochemical alkylation of proteins by diazocyclobutane is possible.

We also considered whether photolysis of diazirine **26** in anhydrous THF would lead to the detectable production of diazocyclobutane **33** upon irradiation at 365 nm. Analogous to experiments above, UV-vis spectroscopy with monitoring at 500–525 nm was used to probe for the formation of diazo compound. Several light sources were tried, as was photolysis at r.t. or –78 °C, but in no case were we able to detect appreciable signal at >500 nm, and while reactions were carried out to completion and monitored at different time points, in no case did we observe the expected pink color associated with diazocyclobutane formation. By contrast, 365 nm irradiation of the linear diazirine **31** in THF produced a peach-colored solution with an absorption at 500 nm attributed to diazo compound **34** (Fig 6F).

Together, these results indicate that 365 nm photolysis of cyclobutanediazirines can produce carbene intermediates as evidenced by formation of their expected bimolecular and unimolecular products. Diazocyclobutane (**2**), when synthesized from a different precursor, reacts rapidly with water and can serve as a protein alkylating agent. Diazocyclobutane **2** does not undergo photochemistry at 365 nm. Unlike linear diazirines, cyclobutanediazirine **26** does not give detectable amounts of diazo compound **33** upon low temperature photolysis in organic solvent, suggesting that **33** is either not formed or is especially labile.

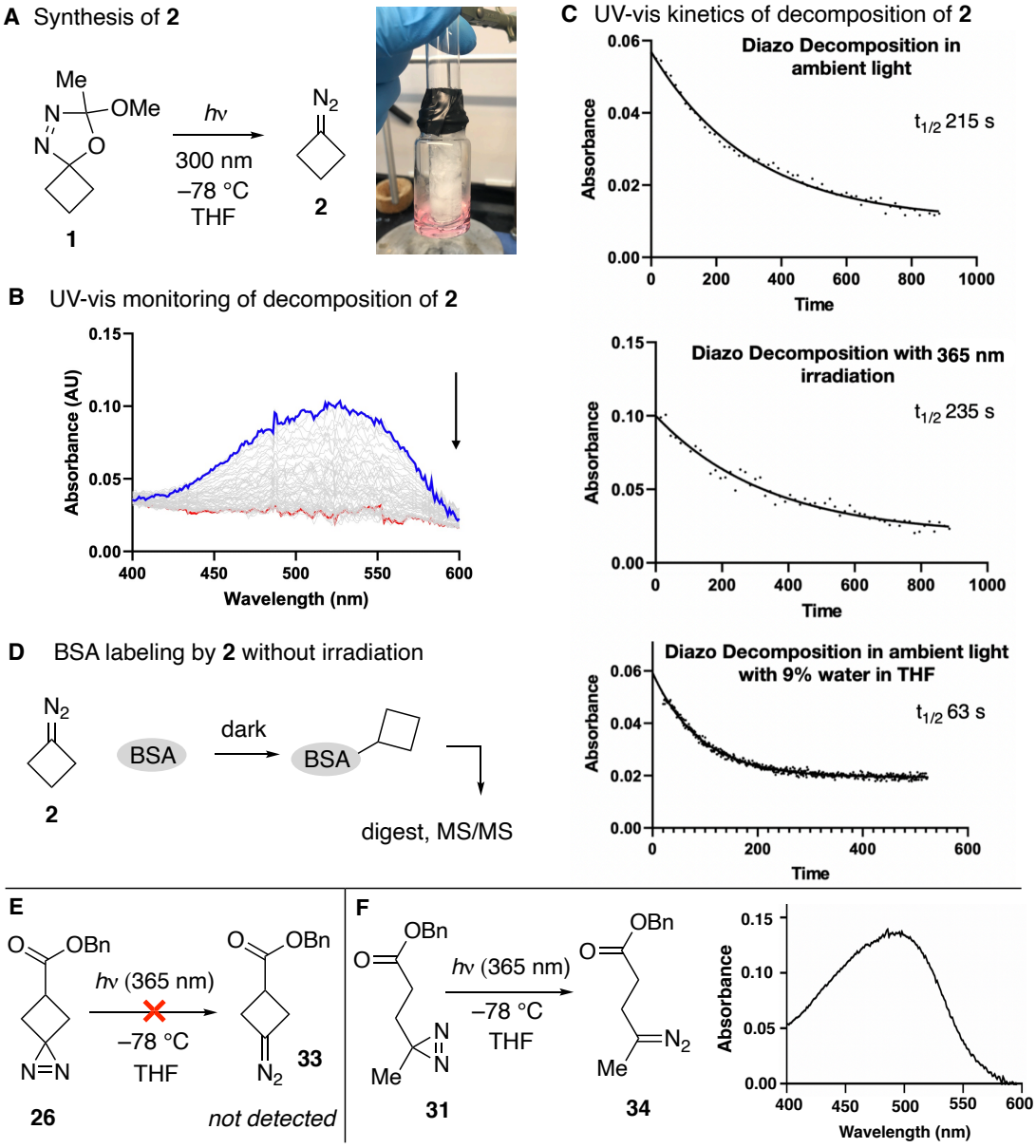

Figure 6 (A) Low temperature photolysis of **1** produces **2** as a pink solution. (B) Thermal decomposition of diazocyclobutane **2** can be monitored by UV-vis through time-course monitoring of disappearance of the characteristic absorbance at 525 nm. (C) The rate of decomposition of **2** is unaffected by irradiation with UV-A light centered at 365 nm, but is accelarated by the addition of water. (D) Diazocyclobutane **2** labels BSA without irradiation. (E) Irradiation of **26** in THF at –78 °C does not produce appreciable amounts of **33**, whereas (F) similar irradation of **31** produces **34** as a pink solution with absorbance at 500 nm in the visible spectrum.

Comparative Studies of Linear and Cyclobutanediazirine Probes in Live Cells

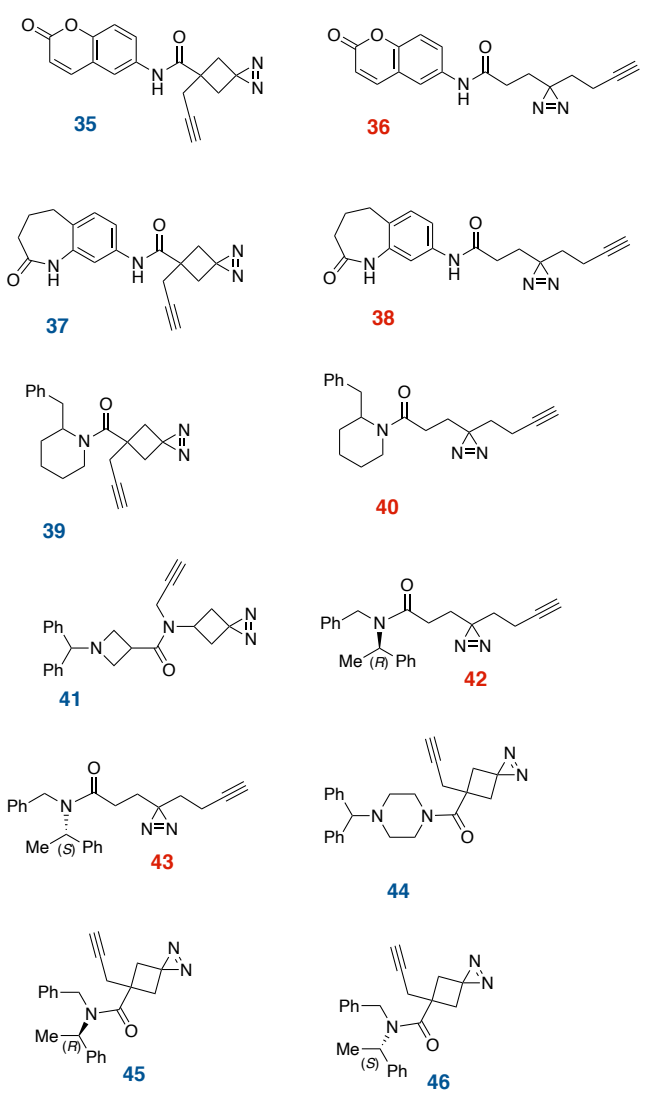

Figure 7. Diazirine probes used for live cell labeling

We next comparatively assessed the general proteomic profiles for a number of linear and cyclobutyl diazirine-based fragment probes[13, 54] derived from coumarin (**35** and **36**), tetrahydro-1-benzazepin-2-one (**37** and **38**), 2-benzylpiperadine (**39** and **40**), α,α-diphenylmethylazetidine-3-carboxamide (**41**), methyl benzylamine (**42**, **43**, **45**, **46**), and benzhydrylpiperazine (**44**, Fig. 7). We first profiled the interactions of these probes via in-gel fluorescence imaging. Briefly, HEK293T cells were treated with the probe compounds at a range of concentrations for 30 min, before UV irradiation (365 nm, 4 °C, 20 min). The cells were then lysed, and the protein-bound probes were ligated to tetramethylrhodamine through a copper-catalyzed azide-alkyne 1,3-dipolar cycloaddition reaction. We found, in agreement with Woo and coworkers[47] that the cyclobutanediazirines generally exhibited much less labeling than their linear counterparts (Fig. 8A, S7A). However, when visualized separately, they do show dose- and target group-dependent protein labeling (Fig. 8B).

To further investigate these trends, we compared the profiles of linear and cyclobutyl diazirine via quantitative MS-based proteomics. Here, cells were treated as above and their interactions identified and quantified via TMT-based proteomics, as previously described.[54] To quantify the relative enrichment of each matched probe, we treated cells with probe pairs at different probe concentrations, revealing a much lower median abundance in the samples treated with the corresponding cyclobutanediazirine probe compared to those treated with the linear dialkyl probe (Fig. 8C-E, S7B, C), consistent with gel-based profiles. To determine if these disparate abundances were due to differences in protein affinities, rather than reactivity differences, we examined the enrichment profiles of proteins that display similar apparent binding affinities for the same molecular recognition group (within 20%). Here, we observed, once again, substantially higher signals for interactions captured by the corresponding linear dialkyl probe , which, in aggregate, produced a signal intensity an order of magnitude greater than that of the

cyclobutanediazirine (Fig. 8F, S7D) for proteins of similar apparent affinities. Finally, we note that the cyclobutanediazirine probes exhibited similar decomposition kinetics to the linear diazirine analog and are largely consumed within the timeframe of the labeling experiment (Fig. 8G). Collectively, these data indicate that cyclobutyl diazirine probes possess lower protein capture efficiency relative to their linear dialkyl counterparts in chemoproteomic experiments.

Conclusions

These studies illustrate the differences in the photochemical behavior of linear diazirines and spirocyclic cyclobutanediazirines with the latter exhibiting a larger contribution from carbene chemistry and a reduced contribution of diazo chemistry. Suggestive of a contributing carbene mechanism, 365 nm irradiation of cyclobutanediazirines produces methylenecyclopropane products as has been observed in earlier studies of cyclobutylidene formed from non-diazirine precursors.[37, 39-42] Additionally, these photolyses produce relatively high (≥50%) yields of bimolecular adducts with MeOH solvent. Additional support for a trappable carbene intermediate was provided by the observation of [2+1] adduct **30** from the photolysis of **26** with tetramethylethylene.

If the irradiation of cyclobutanediazirines were to produce diazocyclobutane products, they would be rapidly protonated and could be capable of reacting with protein targets. Our experiments show that diazocyclobutane reacts rapidly with water and is capable of alkylating BSA. Our experiments further show that diazocyclobutane can be ruled out as a meaningful precursor to cyclobutylidene under 365 nm photolysis conditions. While irradiation of linear diazirines produces a diazoalkane product, attempts to produce a diazocyclobutane via low temperature irradiation of a cyclobutanediazirine were unsuccessful. The reason that carbene formation is favored may be connected to the stability afforded by the non-classical, transannular bonding in cyclobutylidene and the associated transition state for carbene formation.[43] A model where carbene formation is favored over diazo formation under room temperature, aqueous conditions offers a straightforward explanation for the relatively low labeling yields that are observed in cellular experiments. Thus, linear diazirines can produce relatively long-lived diazoalkanes, which are also capable of labeling proteins, whereas cyclobutanediazirines are proposed to give minimal diazo product and labeling occurs predominantly via a carbene mechanism. This model is consistent with the observations and conclusions about carbene involvement by Woo and coworkers,[47] while providing a more straightforward explanation for the observed reduction in overall labeling in cellular studies as well as the observed production of methylenecyclopropane product in vitro. For applications in proteomics, cyclobutanediazirines provide an alternate tool to conventional, linear dialkyldiazirines that, consistent with a carbene crosslinking mechanism, produce lower levels of overall labeling but also lower levels of background labeling. Given the high reactivity and short lifetime of cyclobutylidene intermediates, cyclobutanediazirines should prove especially useful in applications such as small molecule target identification where a small radius of labeling is an especially important consideration.

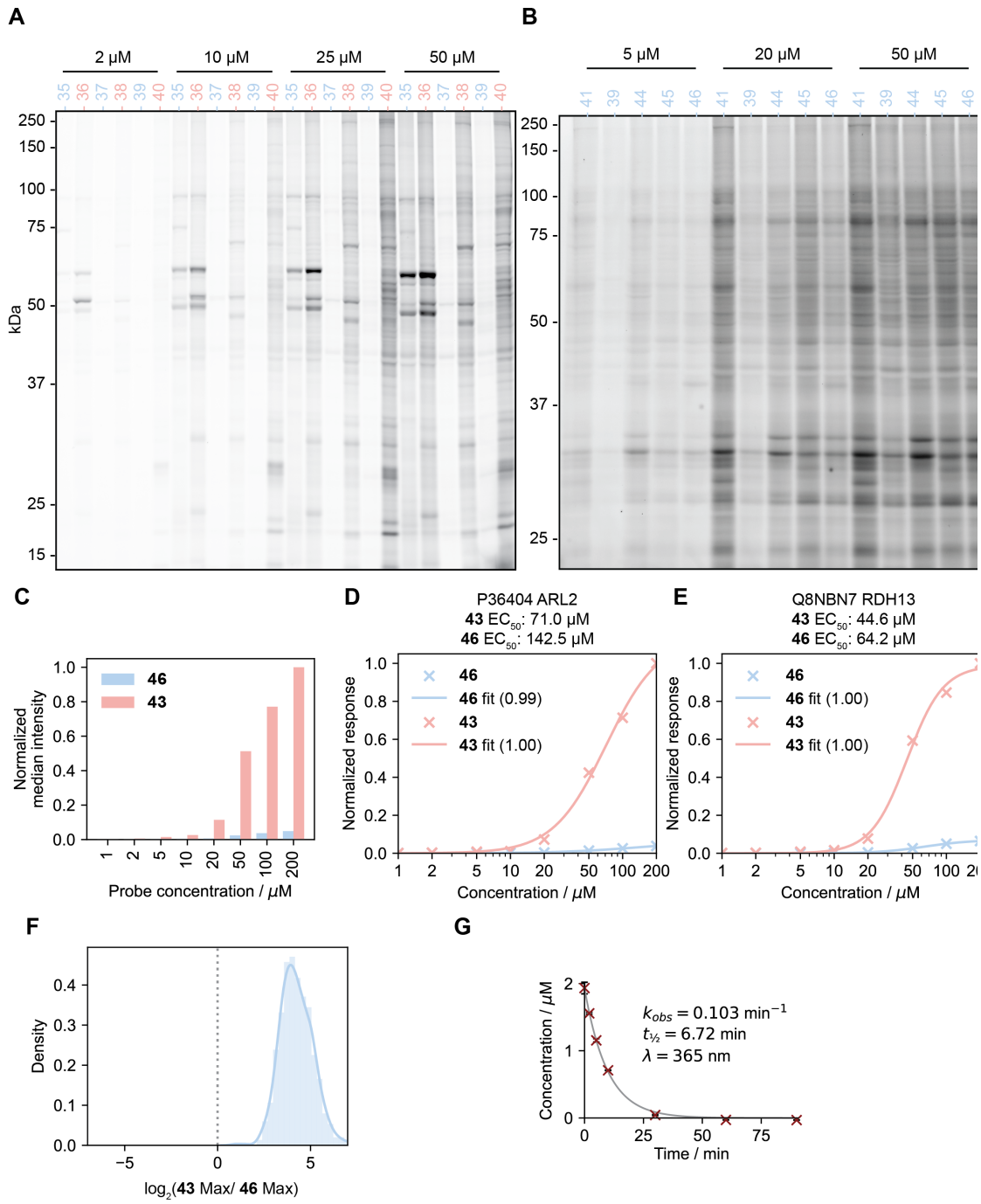

Figure 8. Cyclobutanediazirines exhibit reduced proteomic labeling relative to linear dialkyl diazirines. (A, B) Soluble lysate fraction derived from HEK293T cells treated with cyclobutyl (blue) and linear dialkyl diazirine probes (red) for 30 min followed by UV irradiation (365 nm for 20 min), conjugated to TAMRA-azide, and visualized by in-gel fluorescence. (C) Proteomic median abundances of targets enriched by **43** and **46** at different concentrations. (D, E) Proteomic abundances for representative proteins treated with different concentrations of probes **43** and **46**. (F) Comparing the ratios of maximum intensity for proteins that possess similar **43** and **46** EC_{50} values (within 20 %) shows that the linear dialkyl diazirine probes label proteins with approximately 16-fold greater efficiency. (G) First-order decay of **41** upon UV irradiation (365 nm). Error bars represent standard deviation, n=3.

Author Information

Corresponding Authors

Christopher G. Parker, Department of Chemistry, The Scripps Research Institute, La Jolla, California 92037, United States; Orcid, https://orcid.org/0000-0001-8509-9289; Email: cparker@scripps.edu

Christopher W. am Ende, Pfizer Worldwide Research and Development, Eastern Point Road, Groton, Connecticut 06340, United States; Orcid, https://orcid.org/0000-0001-8832-9641; Email: christopher.amende@pfizer.com

Joseph M. Fox, Department of Chemistry and Biochemistry, University of Delaware, Newark, Delaware 19716, United States; Orcid, https://orcid.org/0000-0002-8258-1640; Email: jmfox@udel.edu

Authors

Jessica O'Brien, Department of Chemistry and Biochemistry, University of Delaware, Newark DE 19716, United States.

Louis P. Conway, Department of Chemistry, The Scripps Research Institute, La Jolla, California

Paramesh Ramaraj, Department of Chemistry and Biochemistry, University of Delaware, Newark DE 19716, United States.

Appaso M. Jadhav, Department of Chemistry, The Scripps Research Institute, La Jolla, California 92037, United States.

Jun Jin, BioDuro-Sundia, No.233 North FuTe Rd., WaiGaoQiao Free Trade Zone, Shanghai, 200131 P.R. China.

Jason K. Dutra, Pfizer Worldwide Research and Development, Eastern Point Road, Groton, Connecticut 06340, United States.

Parrish Evers, Department of Chemistry and Biomolecular Sciences, University of Ottawa, Ottawa, Ontario K1N 6N5, Canada.

Manuel Schupp, Institute of Organic Chemistry, University of Vienna, 1090 Vienna, Austria

Iakovos Saridakis, Institute of Organic Chemistry, University of Vienna, 1090 Vienna, Austria

Yong Chen, Institute of Organic Chemistry, University of Vienna, 1090 Vienna, Austria

Nuno Maulide, Institute of Organic Chemistry, University of Vienna, 1090 Vienna, Austria

John Pezacki, Department of Chemistry and Biomolecular Sciences, University of Ottawa, Ottawa, Ontario K1N 6N5, Canada.

Conflicts of Interest

The authors declare the following competing financial interest(s): J.O'B., J.K.D. and C.W.a.E. are employees of Pfizer Inc; J. J. is an employee of BioDuro-Sundia.

Data availability

The data supporting this article have been included as part of the Supplementary Information.

Acknowledgments

We thank Dr. Yinzhi Fang and Xiyin Lyu for synthetic chemistry support. We thank Didier Bilodeau for experimental assistance with photochemistry experiments. This work was supported by NIH (R01GM132460, J.M.F.), Pfizer (J.M.F.), National Institute of Allergy and Infectious Diseases R01 AI156268 (C.G.P.), Natural Sciences and Engineering Council of Canada #210719 (J. P. P.) and the Austrian Science Fund (FWF, 10.55776/P37182 to N.M.). Instrumentation was supported by NIH awards P20GM104316, P20GM103446, S10OD025185, S10OD026951, S10OD016267, S10OD016361, and S10OD30321. Facilities and instrumentation were also supported by NSF through the University of Delaware Materials Research Science and Engineering Center, DMR-2011824.

References

1. N. R. Burton, P. Kim and K. M. Backus, *Org. Biomol. Chem.*, 2021, **19**, 7792-7809.
2. E. Smith and I. Collins, *Future Med. Chem.*, 2015, **7**, 159-183.
3. A. V. West and C. M. Woo, *Isr. J. Chem.*, 2023, **63**, e202200081.
4. R. A. Homan, J. D. Lapek, C. M. Woo, S. Niessen, L. H. Jones and C. G. Parker, *Nat. Rev. Methods Primers*, 2024, **4**, 30.
5. M. W. Halloran and J. P. Lumb, *Chem. Eur. J.*, 2019, **25**, 4885-4898.
6. A. Herner, J. Marjanovic, T. M. Lewandowski, V. Marin, M. Patterson, L. Miesbauer, D. Ready, J. Williams, A. Vasudevan and Q. Lin, *J. Am. Chem. Soc.*, 2016, **138**, 14609-14615.
7. O. A. Battenberg, M. B. Nodwell and S. A. Sieber, *J. Org. Chem.*, 2011, **76**, 6075-6087.
8. J. B. Geri, J. V. Oakley, T. Reyes-Robles, T. Wang, S. J. McCarver, C. H. White, F. P. Rodriguez-Rivera, D. L. Parker, Jr., E. C. Hett, O. O. Fadeyi, R. C. Oslund and D. W. C. MacMillan, *Science*, 2020, **367**, 1091-1097.
9. A. L. Mackinnon and J. Taunton, *Curr. Protoc. Chem. Biol.*, 2009, **1**, 55-73.
10. Z. Q. Li, P. L. Hao, L. Li, C. Y. J. Tan, X. M. Cheng, G. Y. J. Chen, S. K. Sze, H. M. Shen and S. Q. Yao, *Angew. Chem. Int. Edit.*, 2013, **52**, 8551-8556.
11. J. Gao, A. Mfuh, Y. Amako and C. M. Woo, *J. Am. Chem. Soc.*, 2018, **140**, 4259-4268.
12. J. Tang, W. Li, T.-Y. Chiu, F. Martínez-Peña, Z. Luo, C. T. Chong, Q. Wei, N. Gazaniga, T. J. West, Y. Y. See, L. L. Lairson, C. G. Parker and P. S. Baran, *Nature*, 2023, **622**, 507-513.
13. C. G. Parker, A. Galmozzi, Y. Wang, B. E. Correia, K. Sasaki, C. M. Joslyn, A. S. Kim, C. L. Cavallaro, R. M. Lawrence, S. R. Johnson, I. Narvaiza, E. Saez and B. F. Cravatt, *Cell*, 2017, **168**, 527-541.e529.
14. D. P. Murale, S. C. Hong, M. M. Haque and J. S. Lee, *Proteome Sci*, 2017, **15**.
15. C. X. Song and C. He, *Acc. Chem. Res.*, 2011, **44**, 709-717.

16. M. R. Bond, H. C. Zhang, J. Kim, S. H. Yu, F. Yang, S. M. Patrie and J. J. Kohler, *Bioconj. Chem.*, 2011, **22**, 1811-1823.
17. M. J. Niphakis, K. M. Lum, A. B. Cognetta, 3rd, B. E. Correia, T. A. Ichu, J. Olucha, S. J. Brown, S. Kundu, F. Piscitelli, H. Rosen and B. F. Cravatt, *Cell*, 2015, **161**, 1668-1680.
18. Y. Xia and L. Peng, *Chem. Rev.*, 2013, **113**, 7880-7929.
19. J. Brunner, H. Senn and F. M. Richards, *J. Biol. Chem.*, 1980, **255**, 3313-3318.
20. S. M. Korneev, *Eur. J. Org. Chem.*, 2011, **2011**, 6153-6175.
21. D. A. Modarelli, S. Morgan and M. S. Platz, *J. Am. Chem. Soc.*, 1992, **114**, 7034-7041.
22. J. M. Fox, J. E. G. Scacheri, K. G. L. Jones, M. Jones, P. B. Shevlin, B. Armstrong and R. Sztyrbicka, *Tetrahedron Lett.*, 1992, **33**, 5021-5024.
23. N. Chen, M. Jones, Jr., W. R. White and M. S. Platz, *J. Am. Chem. Soc.*, 1991, **113**, 4981-4992.
24. A. M. Mansoor and I. D. R. Stevens, *Tetrahedron Lett.*, 1966, 1733-&.
25. G. R. Chambers and M. Jones, *J. Am. Chem. Soc.*, 1980, **102**, 4516-4518.
26. K. T. Chang and H. Shechter, *J. Am. Chem. Soc.*, 1979, **101**, 5082-5084.
27. W. Kirmse, T. Meinert, D. A. Modarelli and M. S. Platz, *J. Am. Chem. Soc.*, 1993, **115**, 8918-8927.
28. K. A. Mix, M. R. Aronoff and R. T. Raines, *ACS Chem. Biol.*, 2016, **11**, 3233-3244.
29. C. Iacobucci, M. Götze, C. Piotrowski, C. Arlt, A. Rehkamp, C. Ihling, C. Hage and A. Sinz, *Anal. Chem.*, 2018, **90**, 2805-2809.
30. J. F. Mcgarrity and T. Smyth, *J. Am. Chem. Soc.*, 1980, **102**, 7303-7308.
31. M. Pearce, *Helv. Chim. Acta*, 1980, **63**, 887-891.
32. N. A. McGrath, K. A. Andersen, A. K. Davis, J. E. Lomax and R. T. Raines, *Chem. Sci.*, 2015, **6**, 752-755.
33. K. A. Mix, J. E. Lomax and R. T. Raines, *J Am Chem Soc*, 2017, **139**, 14396-14398.
34. V. T. Ressler, K. A. Mix and R. T. Raines, *ACS Chem. Biol.*, 2019, **14**, 599-602.
35. J. G. K. O'Brien, A. Jemas, P. N. Asare-Okai, C. W. am Ende and J. M. Fox, *Org. Lett.*, 2020, **22**, 9415-9420.
36. A. V. West, G. Muncipinto, H. Y. Wu, A. C. Huang, M. T. Labenski, L. H. Jones and C. M. Woo, *J. Am. Chem. Soc.*, 2021, **143**, 6691-6700.
37. J. P. Pezacki, D. L. Pole, J. Warkentin, T. Chen, F. Ford, J. P. Toscano, J. Fell and M. S. Platz, *J. Am. Chem. Soc.*, 1997, **119**, 3191-3192.
38. S. Morgan, J. E. Jackson and M. S. Platz, *J. Am. Chem. Soc.*, 1991, **113**, 2782-2783.
39. L. Friedman and H. Shechter, *J. Am. Chem. Soc.*, 1960, **82**, 1002-1003.
40. S. Kammula and P. B. Shevlin, *J. Am. Chem. Soc.*, 1974, **96**, 7830-7832.
41. U. H. Brinker and G. Schenker, *Chem. Commun.*, 1982, 679-681.
42. U. H. Brinker and M. Boxberger, *Angew. Chem. Int. Edit.*, 1984, **23**, 974-975.
43. L. L. Stracener, R. J. Halter, R. J. McMahon, C. Castro and W. L. Karney, *J. Org. Chem.*, 2000, **65**, 199-204.
44. T. Nordvik, J.-L. Mieusset and U. H. Brinker, *Org. Lett.*, 2004, **6**, 715-718.
45. IUPAC nomenclature is diazaspiro[2.3]hex-1-ene.
46. O. V. Martyloga, A. Myronenko, A. M. Tkachenko, V. O. Matvienko, Y. O. Kuchkovska and O. O. Grygorenko, *Eur. J. Org. Chem.*, 2019, **2019**, 3744-3750.
47. A. V. West, Y. Amako and C. M. Woo, *J. Am. Chem. Soc.*, 2022, **144**, 21174-21183.
48. H.-P. Guan, Y.-L. Qiu, M. B. Ksebati, E. R. Kern and J. Zemlicka, *Tetrahedron*, 2002, **58**, 6047-6059.
49. A. Misale, S. Niyomchon, M. Luparia and N. Maulide, *Angew. Chem. Int. Edit.*, 2014, **53**, 7068-7073.
50. R. Panish, S. R. Chintala, D. T. Boruta, Y. Fang, M. T. Taylor and J. M. Fox, *J. Am. Chem. Soc.*, 2013, **135**, 9283-9286.
51. E. L. Tae and M. S. Platz, *Tetrahedron Lett.*, 1999, **40**, 2875-2878.
52. R. Bonneau and M. T. H. Liu, *J. Am. Chem. Soc.*, 1996, **118**, 7229-7230.

53. J. P. Pezacki, B. D. Wagner, C. S. Q. Lew, J. Warkentin and J. Lusztyk, *J. Am. Chem. Soc.*, 1997, **119**, 1789-1790.
54. Y. Wang, M. M. Dix, G. Bianco, J. R. Remsberg, H.-Y. Lee, M. Kalocsay, S. P. Gygi, S. Forli, G. Vite, R. M. Lawrence, C. G. Parker and B. F. Cravatt, *Nat. Chem.*, 2019, **11**, 1113-1123.